



# HARP Collaboration

HARP Memo 08-103

8 October 2008

<http://cern.ch/harp-cdp/driftvelocity.pdf>

## The electron drift velocity in the HARP TPC

---

V. Ammosov, A. Bolshakova, I. Boyko, G. Chelkov, D. Dedovitch, F. Dydak, A. Elagin,  
M. Gostkin, A. Guskov, V. Koreshev, Z. Kroumchtein, Yu. Nefedov, K. Nikolaev,  
J. Wotschack, A. Zhemchugov

CERN-HARP-CDP-2008-004  
08/10/2008



### Abstract

Apart from the electric field strength, the drift velocity depends on gas pressure and temperature, on the gas composition and on possible gas impurities. We show that the relevant gas temperature, while uniform across the TPC volume, depends significantly on the temperature and flow rate of fresh gas. We present the correction algorithms for changes of pressure and temperature, and the precise measurement of the electron drift velocity in the HARP TPC.

# Contents

<b>1</b>	<b>Introduction</b>	<b>2</b>
<b>2</b>	<b>Theoretical expectation on drift velocity variations</b>	<b>2</b>
<b>3</b>	<b>The TPC gas</b>	<b>3</b>
<b>4</b>	<b>Drift velocity variation with gas temperature</b>	<b>4</b>
<b>5</b>	<b>Drift velocity variation with gas pressure</b>	<b>6</b>
<b>6</b>	<b>The algorithm for temperature and pressure correction</b>	<b>7</b>
<b>7</b>	<b>Drift velocity variation with gas composition and impurities</b>	<b>9</b>
<b>8</b>	<b>Small-radius and large-radius tomographies</b>	<b>12</b>
<b>9</b>	<b>Comparison with ‘Official’ HARP’s analysis</b>	<b>15</b>

# 1 Introduction

In a TPC, the longitudinal  $z$  coordinate is measured via the drift time. Therefore, the drift velocity of electrons in the TPC gas is a centrally important quantity for the reconstruction of charged-particle tracks.

Since we are not concerned here with the drift velocity of ions, we will henceforth refer to the drift velocity of electrons simply as ‘drift velocity’.

In this paper, we discuss first the expected dependencies of the drift velocity on temperature, pressure and gas impurities. Then we will discuss the methods of measuring the drift velocity, and finally give our results for drift velocities.

A preliminary account of our work was given in our group’s 2005 Status Report to the SPSC [1]. Here, we present an update of this earlier, incomplete, work. First, the dependence on gas pressure that was neglected before, is now taken into account. Second, while dynamic TPC distortions were only approximately corrected before, their precise correction is now finalized. Third, the TPC pad plane temperature that we used earlier as reference, is now recognized as incorrect representation of the TPC gas temperature.

The drift velocity has also been discussed and determined in ‘Official’ HARP’s large-angle analysis [2]. We disagree with their approach and results. ‘Official’ HARP’s approach and results described in the HARP Technical Paper [3] are somewhat improved, however the disagreement with our results persists. We come back to this issue in Section 9.

## 2 Theoretical expectation on drift velocity variations

The electron drift velocity depends on  $E/\rho$ , the ratio of the electric field strength to the gas density (‘reduced electric field’), and through the latter on gas temperature and pressure (see, for example, Ref. [4]).

From a linear expansion of the drift velocity around  $1/\rho_0$ , we obtain

$$v(1/\rho) = v(1/\rho_0) + dv/d\left(\frac{1}{\rho}\right) \cdot \Delta\left(\frac{1}{\rho}\right) = v_0 + S \cdot \Delta\left(\frac{1}{\rho}\right) \quad (1)$$

and

$$\frac{\Delta v}{v} = -\frac{S}{v} \frac{\Delta\rho}{\rho^2}. \quad (2)$$

From the law of ideal gases, the following relation is expected to hold approximately between the relative changes of the gas density, temperature and pressure:

$$\frac{\Delta\rho}{\rho} \simeq \frac{\Delta P}{P} - \frac{\Delta T}{T}, \quad (3)$$

where  $T$  is the absolute gas temperature and  $P$  the absolute gas pressure.

Inserting  $\Delta\rho/\rho$  from Eq. (3) into Eq. (2) gives for the dependence of the relative variation of the drift velocity on relative temperature and pressure changes

$$\frac{\Delta v}{v} \simeq -\frac{S}{\rho v} \left( \frac{\Delta P}{P} - \frac{\Delta T}{T} \right) = -\alpha \left( \frac{\Delta P}{P} - \frac{\Delta T}{T} \right). \quad (4)$$

We note that the same coefficient  $\alpha$  also determines the dependence of the relative variation of the electron drift velocity on the relative variation of the electric field strength:

$$\frac{\Delta v}{v} = \alpha \frac{\Delta E}{E}. \quad (5)$$

### 3 The TPC gas

The HARP TPC was operated with the P9 gas mixture (91% argon and 9% methane by volume) at  $\sim 5$  mbar above the ambient atmospheric pressure (the overpressure was determined by an oil level in a bubbler). The temperature of the gas resulted from the ambient temperature of the experimental hall, from the cooling power of the water-cooled metal sheets which shielded the TPC from the heat of the solenoidal magnet coil, and from the temperature of the incoming fresh gas.

The electric drift field was 111 V/cm, the solenoidal field was 0.7 T. The P9 drift velocity is for these parameters at nominal operating conditions of 760 mm Hg and 30°C temperature at its maximum (see Fig. 1). The purpose of this particular operating condition<sup>1</sup> was to minimize the dependence on small variations of the electric field strength and of the gas density.

At the nominal operating conditions, the MAGBOLTZ prediction [5] of the absolute drift velocity is

$$v = 5.277 \pm 0.016 \text{ cm}/\mu\text{s}. \quad (6)$$

Variations of the drift velocity may arise from deviations from the nominal gas pressure, the nominal temperature, and the nominal gas mixture (for example, a larger methane percentage will increase the drift velocity).

Since the drift velocity is at the nominal operating conditions at or very close to a maximum, the slope  $S$  defined in Eq. (1), while expected to be small in absolute value, may have positive or negative sign.

The MAGBOLTZ prediction of the relative variation of the drift velocity with temperature [5] – at nominal conditions and at constant pressure – is

$$\Delta v/v = +1.9 \times 10^{-4} \Delta T \quad (7)$$

---

<sup>1</sup>The gas mixture and the operating conditions were taken from the experience with the ALEPH TPC.

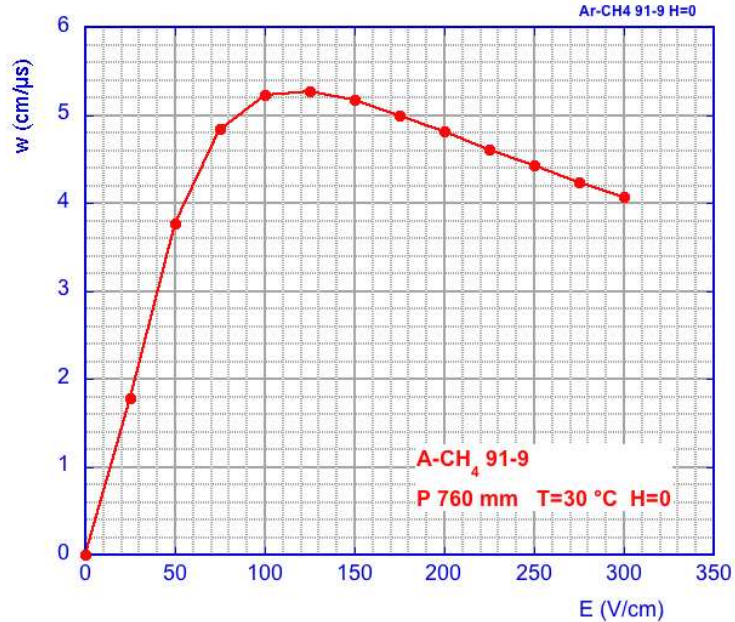


Figure 1: Drift velocity (cm/ $\mu$ s) of the P9 gas as a function of the electric field strength [5].

or

$$\Delta v/v = +5.8 \times 10^{-2} \frac{\Delta T}{T}, \quad (8)$$

where  $T$  and  $\Delta T$  are in degrees Kelvin.

## 4 Drift velocity variation with gas temperature

While the measurement of the absolute drift velocity is non-trivial, its relative variation is much easier to determine. For our study of variations of the drift velocity, we used the reconstructed  $z$ -position of a thin Be target as determined from the extrapolation of tracks back to the target.

The observed variation of the drift velocity (inferred from the apparent variation of the  $z$  target position) from data taken in August 2002 over nearly three days (see the left plot in Fig. 2) shows an unambiguous correlation with the recorded temperature of the TPC's pad plane (see the right plot of Fig. 2). The apparent variation of the target position is at the level of 2 mm.

Figure 2 shows yet another interesting feature: the  $z$  of the target position is larger at the third maximum than at the second maximum, although the temperatures are nearly the same. This effect arises from the concurrent variation of the atmospheric pressure during this data taking period.

Perhaps the most intriguing feature of Fig. 2 is the time delay between the temperature variation of the pad plane and the temperature variation of the drift velocity. In this data

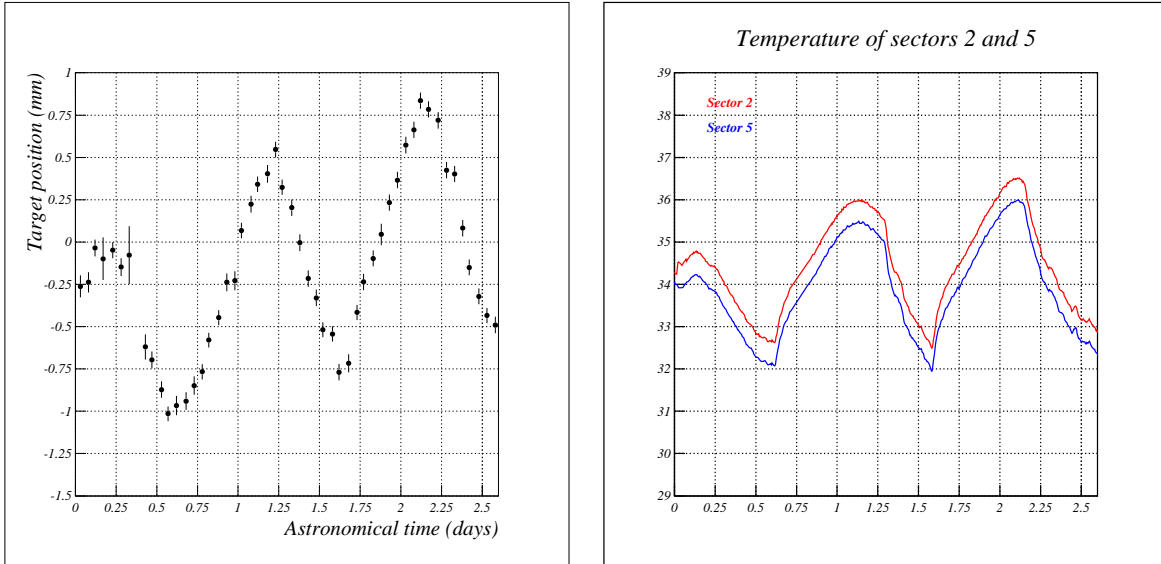


Figure 2: Apparent variation of the  $z$  target position (determined with an assumed drift velocity of  $5.140 \text{ cm}/\mu\text{s}$ ) with time (left panel); temperature of two sectors in the TPC pad plane as a function of time (right panel).

set, it was determined to be about 3 hours (in other data sets, different time delays were found, all several hours long).

What is the origin of the 3 hours delay? To answer this question, we embark on two short digressions.

1. **How long does it take that a 1 degree temperature increase of the pad plane leads to a 1 degree temperature increase of the TPC gas?**

The answer is found from the law of heat flux:

$$d\Phi = -\lambda \cdot dA \cdot \nabla T .$$

For the TPC gas,  $\lambda \approx 0.018 \text{ Wm}^{-1}\text{deg}^{-1}$ . With a heat capacity  $C_p \approx 0.676 \text{ Jg}^{-1}\text{deg}^{-1}$ , a volume of  $7.5 \times 10^5 \text{ cm}^3$ , and a density of  $\rho = 1.69 \times 10^{-3} \text{ g cm}^{-3}$ , 1140 J must be transported through the TPC gas, which needs about 50 hours.

In conclusion, the TPC gas is a very good insulator. It takes a long time to change the gas temperature through temperature changes of the outside envelope of the TPC gas.

2. **How long does it take that a local temperature increase by 1 degree inside the TPC gas leads to a uniform temperature increase across the whole TPC volume?**

The answer is found from Fick's law of the change of a concentration  $c$  by diffusion,

$$\frac{\partial c}{\partial t} = D \cdot \nabla^2 c .$$

For the TPC gas, the diffusion coefficient is  $D \approx 0.16 \text{ cm}^2\text{s}^{-1}$ , therefore any local temperature fluctuation is equalized within seconds across the TPC volume.

In conclusion, the TPC gas represents at any moment a bath of equal temperature across the TPC volume.

It follows that it cannot be the temperature of the TPC envelope that can change the gas temperature on the time scale of a few hours. The only possibility is that the gas temperature changes because the old gas with its old temperature mixes almost instantaneously with the newly incoming gas with its new temperature.

The newly incoming gas passed through  $\sim 100 \text{ m}$  long thin copper pipes across the experimental hall, and therefore adopted closely the ambient temperature of the hall<sup>2</sup>. If the latter changes, notably from day to night, it is the exchange rate of the TPC gas that defines the TPC gas temperature.

Typically, one TPC volume was exchanged every half day, but there were at occasions changes of the flow rate (the flow rate varied between 60 and 120 l/h).

Figure 3 shows, for illustration purposes, a toy model of both the amplitude diminution and the time delay of the TPC gas temperature with respect to the temperature of the experimental hall. For a flow rate of 120 l/h, the delay is about 3 hours. The dependence of the amplitude of the temperature variation on the flow rate is manifest.

Since the delay depends on the exchange rate of the TPC gas, which was changed at specific times, it will be constant in between. The delays can be measured from the apparent variation of the  $z$  target position with respect to the variation of the hall temperature (same procedure as shown in Fig. 2). From the delay the flow rate can be determined and cross-checked against the somewhat fragmentary knowledge of the flow rate from logbook notes (See Table 1 for a summary of the logbook notes). With the known flow rate, it is straightforward to calculate the temperature of the TPC gas as a function of the experimental hall's temperature.

## 5 Drift velocity variation with gas pressure

During data taking, the atmospheric pressure and the TPC gas pressure at the TPC outlet<sup>3</sup> were continuously recorded. The pressure readings are linearly related to the needed absolute pressure.

This linear relation was established with the help of meteorological data recorded at Geneva-Cointrin. Because of occasional signal saturation, only the atmospheric pressure recording turned out to be useful. The detailed analysis of the TPC gas pressure is described in Ref. [6].

The small overpressure of  $\sim 5 \text{ mbar}$  of the TPC gas pressure w.r.t. the atmospheric pressure was ignored<sup>4</sup>.

---

<sup>2</sup>This conclusion is corroborated by the observation that the inlet gas temperature shows the same variation with time as the ambient temperature of the experimental hall.

<sup>3</sup>The 'TPC outlet' position was actually some 15 metres away from the TPC.

<sup>4</sup>The overpressure was constant through all data taking.

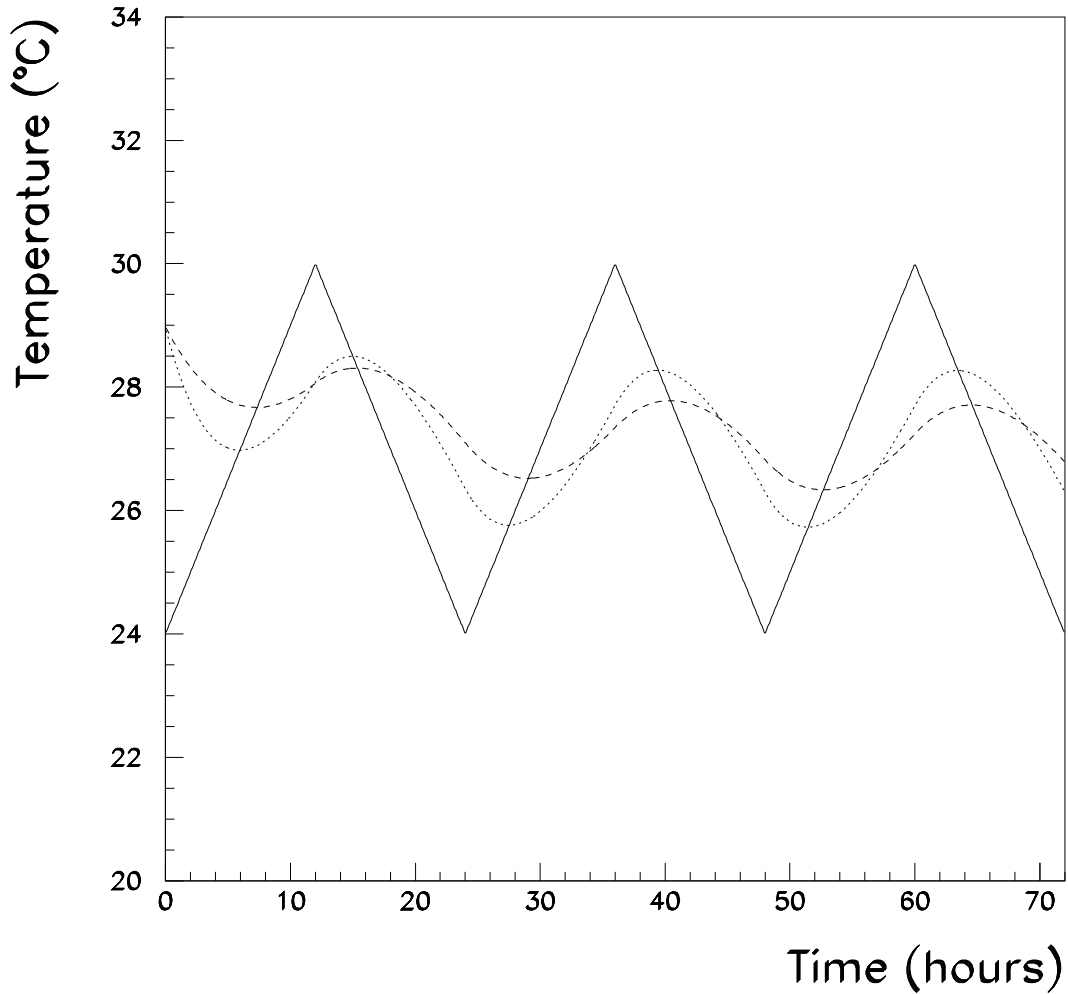


Figure 3: Toy model of the variation of the TPC gas temperature with time; the full line represents the day–night variation of the ambient hall temperature and thus the temperature of the ‘new’ gas; the dashed line shows the TPC gas temperature for a flow rate of 60 l/h, and the dotted line for a flow rate of 120 l/h; in both cases the initial TPC gas temperature is arbitrarily taken as 29°C.

The pressure dependence of the drift velocity has not been experimentally studied *per se*, because of the superposition of the variations with temperature and pressure, and because the relative pressure variation was generally smaller (and less regular) than the relative temperature variation (the day–night regularity of which made its identification much easier).

## 6 The algorithm for temperature and pressure correction

We now determine the proportionality constant  $\alpha$  of Eq. (4) which relates the relative variation of the drift velocity with the difference of the relative variations of temperature and pressure. We take as temperature the *calculated delayed* TPC gas temperature, and as



Table 1: Summary of the logbook notes on setting or changing the TPC gas flow during the 2002 data taking.

Date	Gas flow [litres/hour]	Comment
?	60	
10/05/2002	80	
18/07/2002	120	
?	60	special gas check
24/07/2002	25	krypton calibration
?	60	
04/08/2002	90	
05/08/2002	?	leak on input pipe repaired
09/08/2002	?	gas bottles changed
?	85	
13/08/2002	90	
11/10/2002	110	

pressure the *measured instantaneous* atmospheric pressure:

$$\frac{\Delta v}{v} = -\alpha \left( \frac{\Delta P_{\text{hall}}}{P_{\text{hall}}} - \frac{\Delta T_{\text{TPC}}}{T_{\text{TPC}}} \right) . \quad (9)$$

Before we give the result for  $\alpha$ , we demonstrate the validity of our procedure.

We show in the upper group of four panels in Fig. 4 the measured  $z$  target position as a function of the ‘effective’ TPC gas temperature that is defined as

$$T_{\text{eff}} = (T + 273.15) \cdot (966/P) - 273.15 ,$$

where  $T_{\text{eff}}$  and  $T$  are measured in °C (in other words, small pressure variations are translated into temperature variations). 966 hPa is the average recorded atmospheric pressure. The ‘effective’ TPC gas temperature is calculated with different gas flows ranging from 50 to 200 litres/hour. If the dependence of the measured  $z$  target position on the ‘effective’ TPC gas temperature is approximated as linear, the  $\chi^2$  of straight-line fits will have a minimum at the gas flow that results in a delay of the TPC gas temperature which is in phase with the variation of the  $z$  position. The lower panel in Figure 4 shows that the optimum gas flow is  $85 \pm 5$  litres/hour, in good agreement with the value of 90 litres/hour suggested by logbook recordings.

The lower panel in Figure 5 shows the  $z$  target position as a function of time. The figure’s upper panel shows the *measured* hall temperature and the ‘effective’ TPC gas temperature *calculated* for a gas flow of 90 litres/hour. Unlike the hall temperature, the ‘effective’ TPC gas temperature is well in phase with the variation of the  $z$  target position. We conclude that our model of calculating the TPC gas temperature is correct.

Two remarks are in order.

First, the data comprise a so-called ‘temperature at TPC outlet’. It turned out that this temperature cannot possibly be representative of the temperature of the TPC gas since

it is in phase with the hall temperature, but reduced by an approximate factor of two in amplitude variation. Therefore, we concluded that there must have been a mistake with the connections of temperature sensors. We have discarded these recordings.

Second, the above considerations do not apply to cryogenic targets since the low temperature of these targets created a completely different environment for the TPC gas temperature.

From Eq. (9) we obtained

$$\alpha = -0.27 \pm 0.01 , \quad (10)$$

which means that for a 1 degree *increase* of the ‘effective’ temperature, the drift velocity *decreases* by 0.09 percent.

This dependence is a factor of five stronger than the theoretical prediction of  $\alpha = +5.8 \times 10^{-2}$ , see Eq. (8), and has the opposite sign.

## 7 Drift velocity variation with gas composition and impurities

Molecules are much easier excited by low-energy electrons than atoms of noble gases because of their rich spectrum of rotational and vibrational states. Hence even small admixtures of molecules to a noble gas may have a large impact on the drift velocity.

Specifically, since the threshold for excitation from ground level of the atomic argon atom is more than two orders of magnitude larger than that for the methane molecule, the drift velocity depends critically on the exact argon/methane ratio [7]. The measured dependence on the argon/methane ratio [8] is  $\Delta v/v \simeq +0.03$  for a methane increase from 9 to 10%.

The methane volume content of the pre-mixed gas was specified with a precision of  $9 \pm 0.5\%$ . (measurements of the mixture ratio indicate that the error was smaller by perhaps a factor of two, however we cannot be sure). During the 2002 data taking, new batches of pre-mixed gas were supplied on 5 April, 8 May, 24 June, 9 August, and on 25 September [9], hence we are dealing with five different gas mixtures, with an estimated variation of the drift velocity up to  $\pm 1.5\%$ . Therefore, after due corrections for gas pressure and temperature, we must *a priori* still be prepared for five systematically different drift velocities during the 2002 data taking.

Another danger arises from unwanted admixtures such as water. The water molecule is particularly dangerous since e.g. at 0.1 eV the cross section of excitation by electrons is some three orders of magnitude higher than the respective cross sections of argon and methane.

Water molecules are omnipresent and may have contaminated the TPC gas through pieces of plastic pipes and other materials which are permeable for water and absorb moisture from the environment [10], at a level that we have no way of knowing. Since the humidity of the atmosphere was not constant, we cannot *a priori* exclude some residual variation of the drift velocity due to the ambient humidity in the experimental hall.

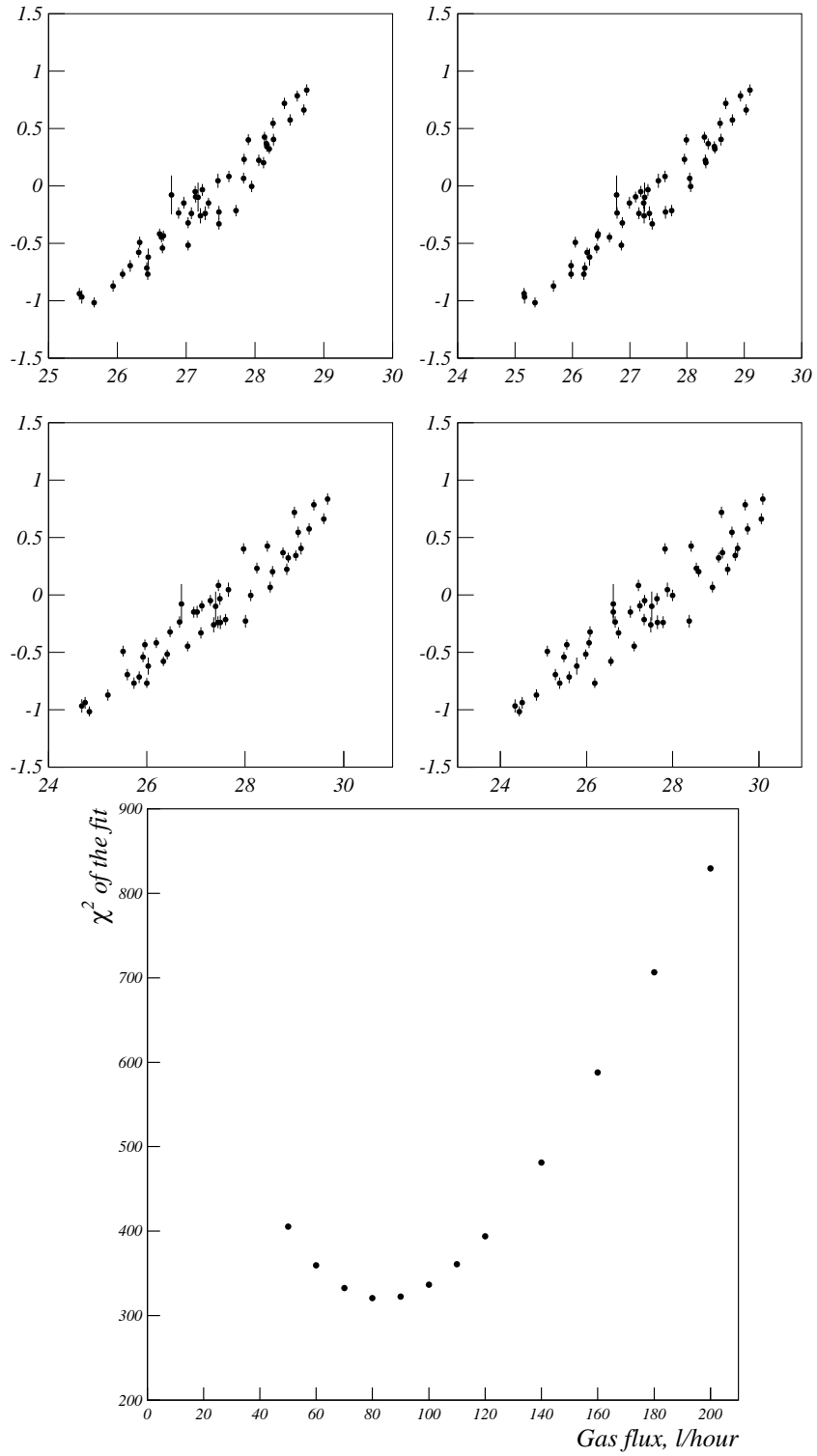


Figure 4: Upper group of four panels: measured  $z$  target position [mm] as a function of the 'effective' TPC gas temperature  $T_{\text{eff}}$ , for assumed gas flows of 60 (upper left), 80 (upper right), 120 (lower left) and 160 (lower right) litres/hour; lower panel:  $\chi^2$  of a linear functional dependence on the 'effective' TPC gas temperature, for different gas flows.

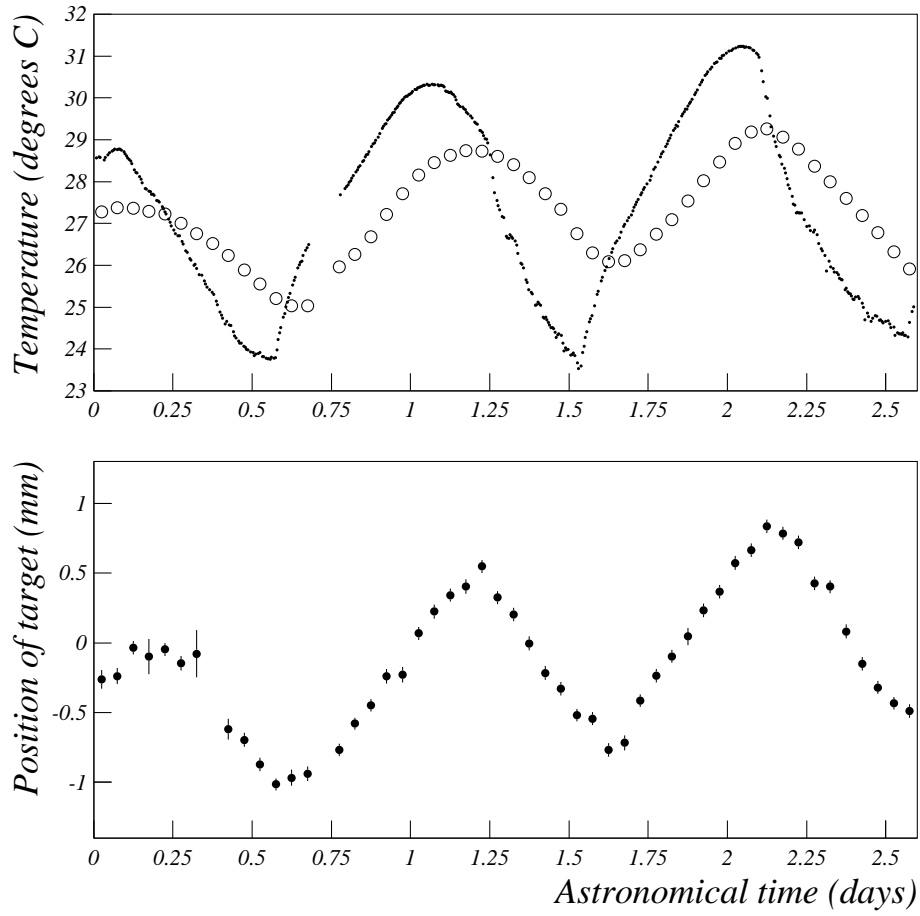


Figure 5: Lower panel:  $z$  target position as a function of time; upper panel: *measured* hall temperature (black points) and the ‘effective’ TPC gas temperature *calculated* for a gas flow of 90 litres/hour (open circles).

## 8 Small-radius and large-radius tomographies

The drift velocity is determined from the difference of the electron arrival times from two points along the  $z$  coordinate inside the TPC whose geometrical position is known from construction. This comparison determines both the drift velocity and a non-zero offset of the  $z$  coordinate.

Systematic errors from two sources must be kept under control for the determination of the drift velocity:

1.  **$z$  coordinate of clusters**

On the average, the reconstructed  $z$  coordinate of clusters must coincide with the trajectory of the physical track. For this reason, we have adopted the **charge-weighted time average of the largest ‘hit’ in a cluster** as the best estimator of the cluster’s  $z$  position<sup>5</sup>, in order to take the largest effect into account, that is the polar-angle dependence of the number of time-samplings. There is also an effect of residual ‘dynamic crosstalk’ which is polar-angle dependent. Both effects, however, will cancel if only tracks through different locations in  $z$  but with **the same polar angle** are considered.

2. **Static and dynamic TPC distortions**

In both static and dynamic TPC distortions, displacements of the  $r \cdot \phi$  coordinate are coupled with displacements of the  $r$  coordinate. Furthermore, both static and dynamic TPC distortions vary strongly across the TPC volume. Therefore, for the reconstruction of the two distinct points along the  $z$  coordinate that serve to measure the drift velocity, a precise correction of TPC distortions is necessary. When only cosmic tracks are used for the determination of the drift velocity, only static TPC distortion corrections are needed. However, cosmic data are not available for all five batches of gas. When using physics tracks, the correction of dynamic TPC distortions also is necessary. In our analysis, both static and dynamic TPC distortions are under control to better than 150 and 300  $\mu\text{m}$ , respectively, throughout the entire TPC volume [11].

Two methods are at disposal to measure the drift velocity which we termed ‘small-radius’ and ‘large-radius’ tomographies.

The small-radius tomography works with tracks that originate from the known position of a thin target, and from the (in principle) known position of the stesalit endcap of the inner field cage that is located downstream of the target. The method has the advantage that tracks of the same polar angle can be compared. It has the disadvantage that the stesalit endcap represents little target material so that the number of tracks is small, that its exact material distribution in the longitudinal  $z$  coordinate is uncertain, and that the distortion of the electric drift field is between these two points larger than anywhere else in the TPC’s tracking volume. When extracting the drift velocity from the reconstructed positions of a thin target and the stesalit endcap, a systematic bias of 1 to 2% is expected if the dependence of  $\Delta v/v$  on  $\Delta E/E$  is not taken into account according to Eq. (5).

---

<sup>5</sup>We recall that a ‘hit’ denotes in a given pad the sequence of charges per time slice.

The large-radius tomography works with tracks that originate from a thin target and hit the geometrically well-defined borders between barrel RPC pads in the  $z$  direction. The signature of such a hit is a good RPC timing signal in two adjacent pads, with no other RPC hit nearby.

The large-radius tomography involves the comparison of tracks with different polar angles, which is a disadvantage. In our view, this is outweighed by three advantages: (i) the positions of the seven points in  $z$ , spaced by 240 mm, provide a much larger lever arm than the single 268.5 mm distance between the centres of the target and the stesalit endcap; (ii) the seven points permit to test the expectation that the drift times versus the  $z$  positions satisfy a straight-line fit; and (iii) the spacing of 240 mm and their positions in space are known with high precision.

We consider the result from the large-radius tomography as the correct one, for its systematic superiority. It results in a driftvelocity that is valid in a large fraction of the TPC's drift volume. We modify this driftvelocity, though, according to local static and dynamic distortions of the electric field. This way, we obtain correct  $z$  positions of clusters everywhere, in particular also in the difficult small-radius region.

For illustration, we give in Tables 2 and 3 results for the cases that a constant drift velocity is determined, i.e., its dependence on electric field distortions is ignored.

In Table 2 we compare the relative drift velocities  $v/v_{\text{ref}}$  and the  $z$  offsets from small-radius and large-radius tomographies in four different data sets (the reference drift velocity,  $v_{\text{ref}} = 5.140 \text{ cm}/\mu\text{s}$ , is used for historical reasons). The quoted errors are for the small-radius tomography statistical only, while for the large-radius tomography the systematic error is included. It is evident that the tomographies at small and large radius show a consistent

Table 2: Relative drift velocities  $v/v_{\text{ref}}$  and  $z$  offset [mm] from large-radius and small-radius tomographies in four different data sets.

		thinBe+8.9	thinBe-8.0	thinTa+3.0	thinTa+5.0
T [°C]		27.3	26.7	27.6	27.0
$v/v_{\text{ref}}$	large radius	1.0145(8)	1.0100(8)	0.9992(8)	0.9952(8)
$z$ offset [mm]		17.0(8)	16.2(8)	15.9(8)	15.1(8)
$v/v_{\text{ref}}$	small radius	1.0077(1)	1.0018(3)	0.9914(3)	0.9891(5)
$z$ offset [mm]		13.8(1)	13.0(1)	12.5(1)	12.9(1)

bias with respect to each other.

To put into perspective the size of the bias, we show in Table 3 a comparison between the nominal and the reconstructed positions of the centres of the target and the stesalit endcap, using the drift velocity obtained from the large-radius tomography. While the nominal and the reconstructed target positions are in reasonable agreement, the nominal and reconstructed stesalit endcap positions are not<sup>6</sup>.

---

<sup>6</sup>The discrepancy diasappears when the dependence of the drift velocity on the electric field distortions, which are largest at the position of the stesalit endcap, is taken into account.

Table 3: Nominal and reconstructed positions [mm] of the centres of the target and of the stesalit endcap, in five different data sets.

	Target (nom.)	Target (rec.)	Endcap (nom.)	Endcap (rec.)
thinBe+8.9	0.0	+0.1 ± 0.6	268.5	270.4 ± 0.6
thinBe-8.0	0.0	+0.8 ± 0.6	268.5	271.5 ± 0.6
thinTa+3.0	2.9	+3.4 ± 0.6	268.5	271.1 ± 0.6
thinTa+5.0	2.9	+3.6 ± 0.6	268.5	270.8 ± 0.6
thinH2O+1.5	0.0	-0.7 ± 0.6	268.5	270.5 ± 0.6

Table 4 gives the electron drift velocities for two physics data sets and for one cosmic data set, all taken during the year 2002, normalized to 25°C temperature, 966 hPa pressure, and an electric field of 111.1 V/cm.

We observe differences between drift velocities larger than expected from the quoted errors, likely to be caused by the use of different gas mixtures. There are also small variations of drift velocity between data sets taken with the same gas mixture, likely due to changes of gas humidity.

Table 4: Results for the electron drift velocity, normalized to 25°C temperature, 966 hPa pressure and an electric field of 111.1 V/cm; the stated periods denote the respective use of batches of gas bottles.

Period	8.5.–24.6.02	9.8.–25.9.02	29.9.02–shutdown
Data sets	Thin Be -8.0 GeV/c	Thin Be +8.9 GeV/c	calibration with cosmic
Drift velocity [mm/μs]	51.87 ± 0.06	52.19 ± 0.06	52.16 ± 0.06

The large-radius tomography can also be used with cosmic muons. They go predominantly from top to bottom through the TPC, are as single and practically straight tracks easy to reconstruct, and populate the TPC volume nearly uniformly in the  $z$  coordinate.

The overall error on the drift velocity is estimated at the 0.1% level, arising from uncertainties in the backscattering of particles from the copper coil of the solenoidal magnet. Since an error in the drift velocity causes an error in the polar angle  $\theta$  and hence an error in the momentum, the drift velocity is required to be precise to better than 2%.

We note that our experimentally determined drift velocities differ from the MAGBOLTZ prediction, see Eq. (6), by much more than its stated theoretical error.

## 9 Comparison with ‘Official’ HARP’s analysis

In the first memo by ‘Official’ HARP on the measurement of the drift velocity [2], neither the variation with pressure and temperature, nor the dates of gas exchange, nor the effect of inadequate TPC track distortions was considered. Their Technical Paper [3] acknowledges the temperature and pressure dependence of the electron drift velocity<sup>7</sup>. Rather than understanding the, and correcting for, temperature and pressure dependencies, they work with day-to-day averages. They employ the small-radius tomography. They claim that their drift velocity is known with a precision of 0.2%.

Our studies neither support the ‘official’ procedure nor the claimed precision.

First, the dominant temperature variation is the day–night variation and it is therefore sub-optimal to work with day-to-day averages. Second, rather than introducing unnecessary statistical fluctuations from insufficient statistics in the determination of day-to-day averages, we prefer to understand the physics origin of variations of the drift velocity, and apply corrections according to the relevant gas pressure and temperature, and the known dates of gas exchange. Third, the ‘official’ analysis missed that the large-radius tomography gives a drift velocity different from the one of the small-radius tomography. Fourth, all methods of determining the drift velocity depend critically on the correction of all relevant TPC track distortions, which we maintain to be wrong in the ‘official’ analysis.

**Therefore, we claim that the ‘official’ drift velocity is not at all known to 0.2% but rather biased by an estimated 1–2%.**

## References

- [1] Report of the CERN–Dubna–Protvino group on the analysis of HARP large-angle data (21 June 2005), <http://cern.ch/harp-cdp/2005reporttoSPSC.pdf>
- [2] M. Apollonio *et al.*, Time calibration and evaluation of the drift velocity, HARP Memo 05-002 (29 April 2005), also available at <http://cern.ch/dydak/HARP-Memo-02-2005.pdf> and <http://cern.ch/dydak/HARP-Memo-02-2005.App.pdf>
- [3] M. G. Catanesi *et al.*, Nucl. Instrum. Methods Phys. Res. **A571** (2007) 527
- [4] W. Blum and L. Rolandi, Particle Detection with Drift Chambers, Springer Verlag (Berlin, Heidelberg, New York), 1993.
- [5] We wish to thank F. Sauli for pertinent discussions, valuable advice and his MAG-BOLTZ calculation of the drift velocity.
- [6] V. Ammosov *et al.*, Pad equalization and  $dE/dx$  in the HARP TPC, HARP Memo 06-104 (19 October 2006), <http://cern.ch/harp-cdp/dEdx.pdf>
- [7] We thank R. Veenhof for useful discussions on this subject.

---

<sup>7</sup>After we had published our pertinent discussion in our 2005 Status Report to the SPSC [1]



- [8] Deduced from a MAGBOLTZ calculation in the frame of the STAR experiment, [http://www.star.bnl.gov/STAR/html/tpc\\_1/hard/tpcrings](http://www.star.bnl.gov/STAR/html/tpc_1/hard/tpcrings)
- [9] We thank L. Linssen for her efforts to recover the history of gas bottle changes.
- [10] R.M. Avramidou and R. Veenhof, Dependence of the MDT chambers drift time on the gas mixture, ATLAS Internal Note (17 May 2004).
- [11] V. Ammosov *et al.*, Nucl. Instrum. Methods Phys. Res. **A588** (2008) 294